Enhanced yellow–green photoluminescence from ZnO–SiO_2 composite opal

2004 J. Phys.: Condens. Matter 16 7277

(http://iopscience.iop.org/0953-8984/16/41/009)

INSTITUTE OF PHYSICS PUBLISHING JOURNAL OF PHYSICS: CONDENSED MATTER

J. Phys.: Condens. Matter **16** (2004) 7277–7286 PII: S0953-8984(04)78998-5

Enhanced yellow–green photoluminescence from ZnO–SiO_2 composite opal

Yingling Yang[1], Beifang Yang[1,3], Zhengping Fu[1], Hongwei Yan[1], Wang Zhen[1], Weiwei Dong[1], Linsheng Xia[1], Wenqi Liu[2], Zuo Jian[2] and Fanqing Li[2]

[1] Department of Materials Science and Engineering, University of Science and Technology of China, Hefei, Anhui 230026, People's Republic of China
[2] Structure Research Laboratory, University of Science and Technology of China, Hefei, Anhui 230026, People's Republic of China

E-mail: bfyang@ustc.edu.cn

Received 7 April 2004, in final form 10 August 2004
Published 1 October 2004
Online at stacks.iop.org/JPhysCM/16/7277
doi:10.1088/0953-8984/16/41/009

Abstract

A remarkably enhanced yellow–green photoluminescence (PL) was observed from ZnO nanocrystals infiltrated into SiO_2 opal photonic crystals. It was clearly visible to the naked eye under the excitation of an Xe lamp and had substantially improved thermal stability over pure ZnO nanocrystals. The PL spectrum shape of a ZnO–SiO_2 composite opal can be modified by annealing an SiO_2 opal or choosing an SiO_2 opal with different lattice parameters. The enhancement of PL intensity is interpreted based on the dependence of the PL intensity on the size of SiO_2 microspheres as well as the anisotropy of the photoluminescence excitation (PLE) spectra. Our results may be interesting for further application.

1. Introduction

The wide-bandgap semiconductor ZnO is a versatile material with many applications including transparent electrodes, antireflection coatings in solar cells [1], varistors [2], gas sensors [3] and electro-luminescence and photo-luminescence devices [4]. At present the luminescence efficiency, the functionality and the stability of ZnO nanocrystals are still required to be substantially improved for applications. Recently, surface-modified ZnO nanoparticles or ZnO nanoparticles introduced into a different matrix were found to show an enhanced PL and to have an improved time stability [4–6].

Photonic crystals (PCs), with periodically dielectric variations, can result in the development of a spectral gap that blocks certain frequencies of photons. PC composite

[3] Author to whom any correspondence should be addressed.

materials are currently attracting much attention for their possible applications, and the physics associated with the interaction between their framework and electromagnetic radiation [7]. Integrating light sources such as semiconductor nanocrystals with artificial opal is a promising method to modify the visible part of the spectrum [8]. Nanocrystals embedded in a PC system also provide a model system for the validation of recent theoretical work [9].

Disorder is always present in artificial PC structures and causes considerable random scattering which strongly influences the optical spectra. However, current research is mainly focused on fabrication and optical characterization of stop-bands and there are only a few experimental reports concerning the effect of random scattering [10].

The aim of this work is to prepare assemblies of ZnO nanocrystals with SiO_2 opals and to investigate the structural effects of the imperfect opal crystals on optical performance in these systems. A simple dipping method was employed to attach ZnO nanocrystals to SiO_2 opal by taking advantage of capillary forces. We chose SiO_2 opal as a host matrix because of its several advantages. SiO_2 is transparent in the visible region and it plays the role of separating ZnO nanocrystals [5]. The separation can be controlled by simply changing lifting speed or concentration of the ZnO nanocrystal ethanol suspension. We observed a remarkably enhanced and modified yellow–green PL in ZnO–SiO_2 composite opal, which had a substantially improved thermal stability over pure ZnO nanocrystals. It is suggested that random scattering has a great influence on PL from ZnO–SiO_2 composite opal.

2. Experiment

ZnO nanocrystals were prepared by the sol–gel method according to the previous report [11]. All chemicals, $Zn(CH_3COO)_2{\cdot}2H_2O$, $LiOH{\cdot}H_2O$ and ethanol, were used as received without further purification. After being aged for several days, the ZnO nanocrystals were washed with heptane, and then the nanocrystals were preserved in alcohol. Nearly monodisperse SiO_2 microspheres with diameters of 205, 245 and 295 nm were synthesized by hydrolysing chemical grade tetraethyl orthosilicate (TEOS) [12]. The SiO_2 opal films on glass microslides were fabricated by using the spontaneous crystallization of monodisperse silica spheres into close-packed arrays via the vertical deposition technique [13]. The annealed SiO_2 opals were obtained through sintering the above samples at various temperatures for 3 h. ZnO nanocrystal infiltrated films were obtained by immersing the SiO_2 opal films into a ZnO nanocrystal ethanol suspension with a volume fraction of 1% and then lifting out at a constant speed of 5 mm min^{-1}. For comparison, bare ZnO nanocrystal film on a glass microslide was also deposited in the same way.

SiO_2 sphere diameters and ZnO–SiO_2 opal morphologies were characterized using a JSM-6700F field emission scanning electron microscope (SEM). X-ray diffraction was measured by a D/max-rA rotating anode x-ray diffractometer with graphite monochromatized Cu Kα radiation. The transmittance measurement was carried out with a UV–vis-365-type spectrometer. The PL spectra and PLE spectra were obtained on an H-850 fluorescence spectrophotometer using a 30 W Xe lamp as the excitation light source. The x-ray photoelectron spectra (XPS) measurements were carried out on a VGESCALAB mark II spectrometer. All the measurements were conducted at room temperature.

Hereafter we label the sample of ZnO nanocrystals infiltrated into as-grown SiO_2 opal with sphere diameter $D = 205$ nm as A1. Similarly, B1 is the sample of ZnO nanocrystals infiltrated into SiO_2 opal with $D = 245$ nm and C1 is that of ZnO nanocrystals infiltrated into SiO_2 opal with $D = 295$ nm. C2 and C3 are the samples of ZnO nanocrystals infiltrated into annealed SiO_2 opals ($D = 295$ nm) that have been sintered at 300 and 700 °C respectively. The bare ZnO film on a glass microslide, which was prepared in the same way as sample C1,

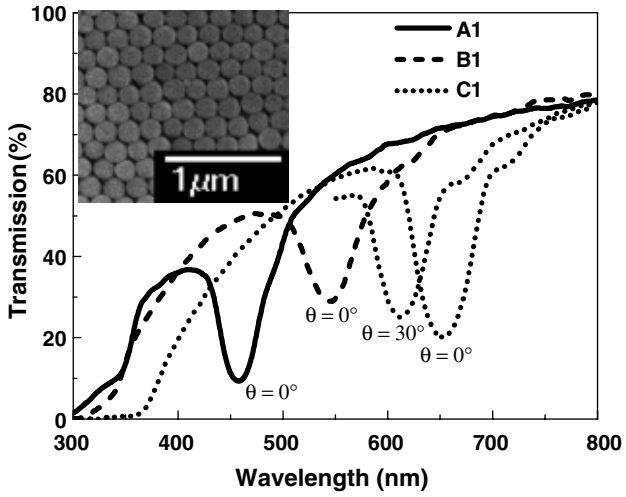

Figure 1. The optical transmission of samples A1 ($D = 205$ nm), B1 ($D = 245$ nm) and C1 ($D = 295$ nm) for different incidence angles (θ) with respect to the surface normal. The incidence angle is indicated in the figure. The inset is the SEM image of sample A1.

is named D1. An approximately 30 μm thick film of ZnO nanocrystals, named D2, was also fabricated by vaporizing a ZnO nanocrystal ethanol suspension at room temperature.

3. Results and discussion

The optical transmission spectra recorded for ZnO–SiO_2 opal composite samples with different SiO_2 sphere diameters are shown in figure 1. These spectra were collected in directions corresponding to different angles, $\theta = 0°$ and 30°, with respect to the normal to the sample surface, while maintaining equality between the angles of incidence and transmission. A clear dip in the optical transmission is observed in each case due to Bragg reflection. For 0° incidence, Bragg reflection moves linearly towards longer wavelengths with the increase of sphere diameter. However, the position of the stop-band shifts to shorter wavelengths as the incident beam angle is increased. All experimental data agree well with the data obtained from theoretical calculations on the basis of Bragg's law:

$$\lambda = 1.632D\sqrt{\varepsilon_{\text{eff}} - \sin^2\theta},$$

where ε_{eff} is the effective dielectric constant (fitting gives 1.85) and D is the sphere diameter. The 'red-shift' of the Bragg dip in the ZnO–SiO_2 composite opal, to 655 nm, as compared with the 650 nm peak position for SiO_2 opal, is caused by the increase of the average dielectric constant. We estimate that the volume fraction of ZnO nanocrystals in composites is $\sim$1% from 'red-shift' by Bragg's law. The inset of figure 1 reveals a ZnO nanocrystal infiltrated well ordered silica sphere array corresponding to the (111) surface of a face-centred cubic structure. The transmission spectra and SEM image show that there are only a few ZnO nanocrystals in the composites, and the infilling process did not destroy the ordered structure of the SiO_2 opal. The thicknesses of the ordered films are estimated to be approximately 5 μm by the empirical rule [11]. The average size of the ZnO nanocrystals is evaluated to be about 5–6 nm from x-ray diffraction data, using the Scherrer equation.

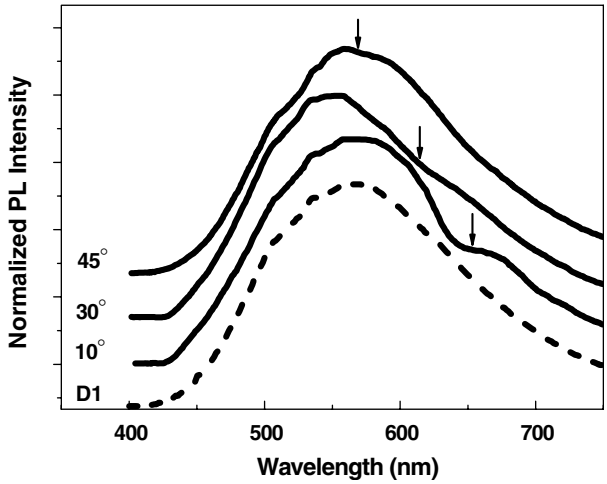

Figure 2. Normalized PL spectra of sample C1 ($D = 295$ nm, solid curve) for different acceptance angles (θ) with respect to the surface normal of the sample. Arrows indicate the position of the centre of the stop-band. The dashed curve is the normalized PL spectra of sample D1 (pure ZnO film). Curves are offset vertically. The curves are normalized such that the magnitude of all peaks is unity.

The PL spectra of all the samples were measured under excitation with 342 nm light. The PL intensity of the pure SiO_2 opal film and the glass microslide is so weak as to be neglected. A broad visible band centred at 565 nm is observed from the PL spectra of the pure ZnO nanocrystal film (figure 2), which is due to a transition of an electron from a level close to the conduction band edge to a deeply trapped hole [14]. During the past years, oxygen vacancies have been assumed to be the most likely candidates for the recombination centres involved in the visible luminescence of ZnO [4, 6, 14]. Dijken *et al* gave further confirmation that the V_o^{**} centre is the recombination centre for the visible emission [14]. The effect of the photonic crystal structure on the PL spectra of the ZnO–SiO_2 opal composites is shown in figure 2, also for a number of observation angles. Relative to the ZnO nanocrystal film, the ZnO nanocrystals infiltrated into the SiO_2 opal (sample C1) exhibit spectral dips in their PL spectra, for example at 650 nm for PL collected at $\theta = 10°$. We indicate in figure 2 with vertical arrows the wavelength of the centre of the stop-band for the angle at which the PL is acquired. The luminescence dip follows the same angular dispersion as the Bragg transmission dip. It has been reported that the optical properties of SiO_2 opal can be modified through thermal treatment [15], which provides an easy way to modify the PL spectrum shape of ZnO–SiO_2 opal composites. When the annealing temperature of the SiO_2 opal is increased, the attenuation band in the yellow–green PL band shifts to shorter wavelengths (figure 3). The blue-shift of the Bragg dip is due to the removal of water and the shrinkage of SiO_2 spheres caused by the heat treatment process [15]. The PL spectrum shape can be modified in a broader range by embedding ZnO nanocrystals in an SiO_2 opal made of spheres with different diameters. Similar to the transmission spectra, the dip in the PL spectra associated with the stop-band moves linearly towards longer wavelengths when the sphere size is increased (figure 4). This shows the modification of the optical properties through sphere size control. It is observed that the dips in PL spectra are much weaker than those in transmission spectra. There are two possible factors concerning this effect.

(1) The course of plane waves through the sample is different from that of fluorescence coming from inside. Unlike transmission stop-bands, the attenuation in the fluorescence

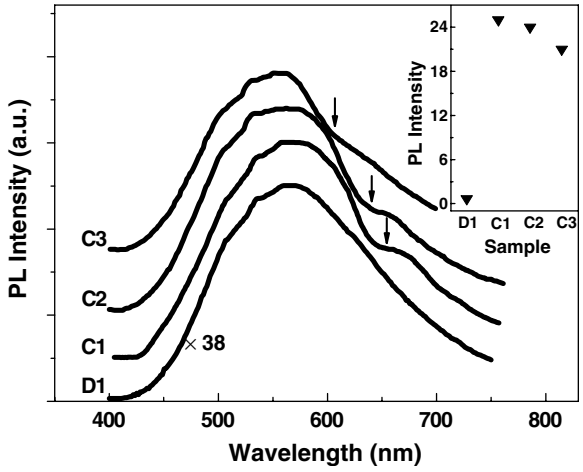

Figure 3. PL spectrum of ZnO nanocrystals infiltrated into annealed SiO_2 opals C1 (as-grown), C2 (300 °C) and C3 (700 °C) and pure ZnO film (D1). Curves are offset vertically. The PL spectra were collected in the direction corresponding to 10°. The inset shows the PL intensity of different samples.

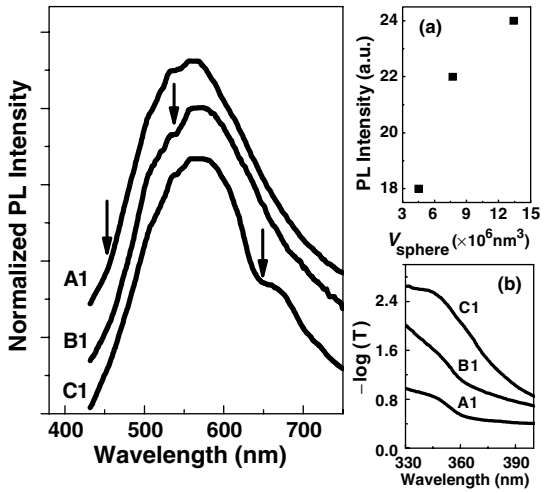

Figure 4. Normalized PL spectrum of samples A1 ($D = 205$ nm), B1 ($D = 245$ nm) and C1 ($D = 295$ nm). Curves are offset vertically. The curves are normalized such that the magnitude of all peaks is unity. The PL spectra were collected in the direction corresponding to 10°. Inset, (a) PL intensity versus microsphere volume ($V_{\text{sphere}} = \frac{\pi D^3}{6}$) in ZnO–$SiO_2$ opal composites. (b) The transmission of samples A1, B1 and C1 at wavelengths from 330 to 400 nm for 0° incidence.

stop-bands is determined primarily by emitters close to the surface but not by those in the bulk of the opals, which results in the fluorescence stop-bands showing much less attenuation [16].

(2) The depth of fluorescence stop-bands is sensitive to the disorder in opals. The disorder introduces a number of defect modes in the stop-band wavelength range and such modes can also be coupled with emitters [17].

It is seen that the broad yellow–green light emission band is markedly enhanced in the ZnO–SiO_2 opal composites from figure 3. The PL intensity of the ZnO–SiO_2 opal composites becomes one order of magnitude higher than that of the pure ZnO nanocrystal film (sample D1). We especially fabricated an approximately 30 μm thick film of ZnO nanocrystals (sample D2), in which the amount of ZnO nanocrystals is three orders of magnitude greater than that of sample C1, but its PL intensity does not even reach half of that of sample C1. This fact confirms that infiltrating ZnO nanocrystals into SiO_2 opal causes an enhancement of PL intensity. It is noteworthy that the peak position and shape of the yellow–green light emission band of the ZnO–SiO_2 opal composites corresponds to that of the ZnO nanocrystals, which implies that the yellow–green emission in the ZnO–SiO_2 composites originates from the same luminescence centres as ZnO nanocrystals. Several factors should be considered as possible reasons for the enhancement of PL intensity in ZnO–SiO_2 opal composites. The factors may include (1) the interfacial coupling between ZnO nanocrystals and unannealed SiO_2 opal; (2) the absorption efficiency of excitation light; (3) the light extraction efficiency.

To reveal the origin of the enhancement of ZnO–SiO_2 composites, we investigated the PL intensity of ZnO nanocrystals infiltrated into annealed SiO_2 opals. The heat treatment will lead to a surface with new physicochemical characteristics which could modify the interfacial interactions [15]. The inset of figure 3 shows there are no distinct variances among the PL intensities of sample C1, C2 and C3. Therefore, the interfacial coupling between ZnO nanocrystals and SiO_2 opals could not be the dominant factor responsible for the intensity enhancement. The XPS measurements also support the above conjecture. The binding energy of the Zn_{2P} electron ($E_{B,2P}$) in the ZnO–SiO_2 opal composites is only 0.1 eV lower than that in pure ZnO nanocrystals, and the kinetic energy of the Auger $Zn_{L3M4,5M4,5}$ electron ($E_{K,LMM}$) in ZnO–SiO_2 is equal to that in pure ZnO nanocrystals. The XPS measurements show that the interfacial interactions between ZnO nanocrystals and SiO_2 opal are weak.

The dependence of the PL intensity on the diameter of SiO_2 microspheres is observed in ZnO–SiO_2 opal composites (inset of figure 4). As SiO_2 microsphere diameter is increased, the PL intensity of the composite is increased. This suggests that multiple scattering of excitation light in the SiO_2 matrix which causes an increase of absorption of excitation light may contribute to the enhancement of PL intensity. Multiple scattering of incident excitation light increases the absorbing probability of photons due to a longer optical path length of incident light in the opals before they exit the samples. Neglecting the reflectance of ZnO–SiO_2 opals (it is small at wavelengths out of the stop-band), the transmission of incident light decreases as the scattering of incident light increases, thus we can characterize approximately the degree of scattering by $-\log T$ (T is transmission). It can be seen from the transmission spectra that the scattering intensity of composites is increased when the SiO_2 microsphere diameter is increased at a wavelength of 342 nm (inset of figure 4). It has been proposed that the scattering in opal is mainly caused by disorder [18]. The disorder in opal was determined by the particle size distribution and the evaporation rate of the suspending solution of SiO_2 spheres [13]. In the case of the same self-assembly conditions and the same relative standard deviations of sphere diameters ($\sigma \approx 5\%$, based on SEM images), the defect concentrations of ordered samples, ratios of defect number to sphere number in the same volume, is considered to show no distinct difference. Thus we can assume the number density of these defects is [18]

$$\rho \propto n = 0.74/V_{\text{sphere}} \propto \frac{1}{V_{\text{sphere}}},$$

where n is the number density of SiO_2 spheres and V_{sphere} is the volume of an SiO_2 sphere. Apparently, the volume of the defect $V_{\text{defect}} \propto V_{\text{sphere}}$. It was proved that lattice periodicity fluctuations give rise to Rayleigh scattering [18], hence the Rayleigh approximation is

tentatively applied to estimate the scattering cross section of a defect

$$S_{sc} \propto V_{defect}^2 \propto V_{sphere}^2.$$

So the intensity of scattering light of opals in the same volume is

$$I_{sc} \propto \rho S_{sc} \propto \frac{1}{V_{sphere}} V_{sphere}^2 \propto V_{sphere} \propto D^3.$$

It can be written as

$$I_{sc} = k^* I_0 D^3,$$

where k^* is a proportionality constant, and I_0 is the incident light intensity. Incident light is reflected, scattered and absorbed by ZnO–SiO_2 opals; only the light absorbed by ZnO nanocrystals contributes to light emission. The observed luminescence intensity can be expressed as

$$O = K\Phi F I$$

where O is the observed luminescence intensity when the sample is being irradiated with an incident intensity of I. Φ is the luminescence quantum yield, F is the fraction of incident light absorbed by ZnO nanocrystals and K is a proportionality constant. The volume fractions of ZnO nanocrystals in composite samples are approximately equal to each other ($\sim$1%), and then by neglecting the contributions of scattering there should be no difference of fluorescence intensity among ZnO–SiO_2 opals with different diameters under the same conditions. Therefore,

$$O_1 = K_1 \Phi F I_0$$

where O_1 is the fluorescence intensity after neglecting the contributions of scattering light. The scattering light can be regard as a new excitation light source and also contribute to yellow–green fluorescence. So the intensity of fluorescence excited by scattered photons is

$$O_2 = K_2 \Phi F I_{sc} = K_2 \Phi F k^* I_0 D^3.$$

In this case, the total intensity of yellow–green fluorescence could be approximately expressed as

$$O_{total} \approx O_1 + O_2 = K_1 \Phi F I_0 + K_2 \Phi F k^* I_0 D^3.$$

It can be seen that the PL intensity is increased when the SiO_2 microsphere diameter is increased. This offers a tentative explanation for the relation between the PL intensity and SiO_2 microsphere diameter. There is a slight departure from a linear relation between the fluorescence intensity and SiO_2 sphere volume ($V_{sphere} = \frac{\pi D}{6}^3$) in our experiment (figure 4), which may be caused by our oversimplified model. The size dependence is expected by Rayleigh scattering in which $D/\lambda \to 0$ is taken for granted. In fact, the bigger the scatterers are, the stronger the departure from the Rayleigh scattering regime is and the less the scattering light intensity shows power exponent dependence on the particle diameter [19]. In addition, there should be two kinds of disorder to be considered in opal [18]:

(1) lattice periodicity fluctuations (deviations of the position and/or size of opal spheres from their exact position and/or size in the perfect crystal lattice; the average dimension of these scatterers is about $0.05D$(10–15 nm));
(2) missing balls, interstitials (the average dimension of these scatterers is about D(200–300 nm), and the Rayleigh approximation is inappropriate for scatterers in this dimension range).

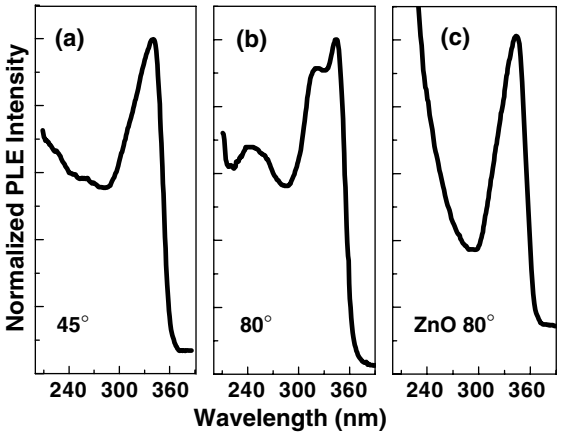

Figure 5. Normalized PLE spectra of sample A1 ($D = 205$ nm) which were measured by monitoring the yellow–green emission band. The curves are normalized such that the magnitude of all peaks is unity. These spectra were obtained for incidence angles corresponding to 45° and 80°, with respect to the normal to the sample surface. The PLE spectra of sample D1 (pure ZnO film) for 80° is also shown.

The anisotropic PLE spectra of ZnO–SiO_2, which were measured by monitoring the yellow–green emission band, provide further evidence that scattering of incident light influences their PL spectra (figure 5). These spectra were obtained for incidence angles of the exciting beam corresponding to 45° and 80°, with respect to the normal to the sample surface. The anisotropic PLE spectra are not observed from pure ZnO nanocrystal film. We know that there is an angle dependence in the scattering process [19], and the intrinsic process of photoluminescence does not change with the incidence angle of the excitation light. Therefore, the anisotropic PLE spectra are probably caused by the interaction between excitation light and the ZnO–SiO_2 opal matrix.

Another factor causing the emission enhancement may be the improvement of the light extraction efficiency of the ZnO–SiO_2 opal film. Recently, an increase in the device coupling-out factor for electroluminescent efficiency by using the scattering structure has been demonstrated [20]. In that research, closed-packed arrays of silica microspheres were incorporated into organic light-emitting devices and acted as a light scattering medium for the light propagated in waveguiding modes within the device. The observation also demonstrated the high scattering efficiency of the ordered array of silica microspheres. Usually, the improved extraction could lead to an intensity enhancement of no more than one order of magnitude.

The incident wavelength is far away from the stop-bands; we supposed that the PL enhancement is not directly related to photonic stop-band structure. A supplemental experiment was adopted in which ZnO–SiO_2 disordered film was synthesized by infiltrating ZnO nanocrystals into the SiO_2 disordered system. The SiO_2 disordered system was obtained by ultrasonically mixing ethanol colloidal suspensions of SiO_2 microspheres with different diameters (205, 245 and 295 nm) and then dropping the mixture on a glass microslide. An enhancement of PL intensity by one order of magnitude was also observed in the disordered sample. The fact indicates that the PL enhancement is mainly attributable to the random scattering of disorder.

It is also found that the yellow–green emission exhibited by the ZnO–SiO_2 composites is more stable: the position and shape do not change after being annealed at 150 °C while the ZnO nanocrystal film is found to undergo a significant red-shift (figure 6). The green

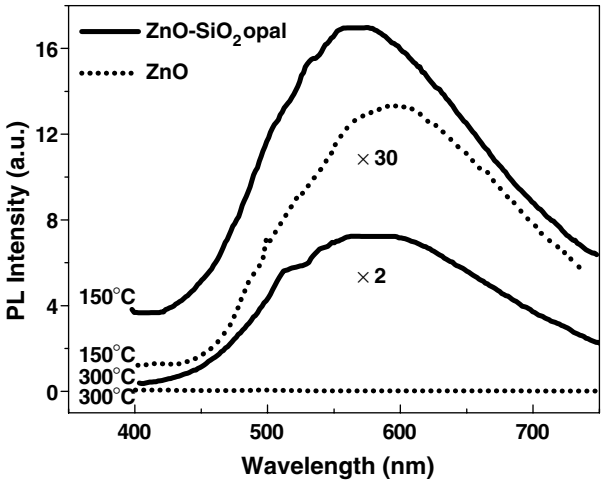

Figure 6. PL spectrum of ZnO–SiO_2 opal composite (solid curve) and nanocrystalline ZnO (dotted curve) that have been annealed at 150 and 300 °C in air for 2 h respectively. Curves are offset vertically.

emission is quenched from the pure ZnO nanocrystal film that was annealed at 300 °C in the air for 2 h, while it is also observed from the ZnO–SiO_2 composites though the intensity decreases (figure 6). Thus, the ZnO–SiO_2 composite has an improved stability over pure ZnO nanocrystals. The previous research has proved that emission properties of ZnO nanocrystals are sensitive to particle size and numbers of oxygen vacancies [14, 21]. Indeed, the surface of SiO_2 microspheres composed by smaller SiO_2 nanoparticles contains pores with a size of about 5 nm which is very close to the average size of ZnO nanoparticles [5]. This fact implies that the ZnO nanoparticles in ZnO–SiO_2 composites can occupy those pores so that they are separated only by SiO_2 primary particles, and the growth and aggregation of ZnO nanocrystals in the heat treatment progress are avoided. On the other hand, addition of enough oxygen in the heat treatment progress may be suppressed for ZnO–SiO_2 composites due to lack of oxygen in the pores [4], which prevents numbers of oxygen vacancies in nano-ZnO particles from decreasing. As a result, the temperature stability was improved when ZnO nanocrystals were embedded in SiO_2 opal. In addition, we observed that the time stability of ZnO–SiO_2 composites was also improved. A similar phenomenon has been reported by Mikrajuddin *et al* [5].

4. Conclusion

In summary, we have developed a method for obtaining intense yellow–green emission of ZnO nanocrystals by infiltrating ZnO nanocrystals into SiO_2 opal. ZnO–SiO_2 opal samples exhibit spectral dips in their PL spectra, which is ascribed to the photonic stop-band effect. The results also show a modification of the optical properties resulting from annealing or sphere size control. Although the volume fraction of ZnO nanocrystals in the composites is very small, their yellow–green emission is clearly visible to the naked eye under the excitation of a 30 W Xe lamp. The enhancement of PL intensity is ascribed to the disorder scattering in opals that increases the excitation light absorption efficiency and the light extraction efficiency. It is also found that the ZnO–SiO_2 composites have an improved temperature stability over pure ZnO nanocrystals.

Acknowledgments

This work is supported by the China National Natural Science Research Foundation. The authors thank Professor Liren Lou for useful discussions.

References

[1] Chopra K L and Das S R (ed) 1983 *Thin Film Solar Cells* (New York: Plenum)
[2] Kong L B, Li F, Zhang L Y and Yao X 1998 *J. Mater. Sci. Lett.* **17** 769
[3] Muller J and Fresenius S W 1994 *J. Anal. Chem.* **349** 380
[4] Mo C M, Li Y H, Lin Y S, Zhang Y and Zhang L D 1998 *J. Appl. Phys.* **83** 4389
[5] Mikrajuddin, Iskandar F, Okuyama K and Shi F G 2001 *J. Appl. Phys.* **89** 6431
[6] Guo L, Yang S H, Yang C L, Yu P, Wang J N, Ge W K and Wong G K L 2000 *Appl. Phys. Lett.* **76** 2901
Li J F, Yao L Z, Ye C H, Mo C M, Cai W L, Zhang Y and Zhang L D 2001 *J. Cryst. Growth* **223** 535
Fu Z P, Yang B F, Li L, Dong W W, Jia C and Wu W 2003 *J. Phys.: Condens. Matter* **15** 2867
[7] Galisteo-Lopez J F, Lopez-Tejeira F, Rubio S, Lopez C and Sanchez-Dehesa J 2003 *Appl. Phys. Lett.* **82** 4068
[8] Petrov E P, Bogomolov V N, Kalosha I I and Gaponenko S V 1998 *Phys. Rev. Lett.* **81** 77
Lin Y, Zhang J, Sargent E H and Kumacheva E 2002 *Appl. Phys. Lett.* **81** 3134
[9] Woldeyohannes M and John S 2003 *J. Opt. B: Quantum Semiclass. Opt.* **5** R43–82
John S and Florescu M 2001 *J. Opt. A: Pure Appl. Opt.* **3** S103
[10] Koenderink A F and Vos W L 2003 *Phys. Rev. Lett.* **91** 213902
[11] Spanhel L and Anderson M A 1991 *J. Am. Chem. Soc.* **113** 2826
[12] StÖber W, Fink A and Bohn E 1968 *J. Colloid Interface Sci.* **26** 62
[13] Jiang P, Bertone J F, Hwang K S and Colvin V L 1999 *Chem. Mater.* **11** 2132
[14] van Dijken A, Meulenkamp E A, Vanmaekelbergh D and Meijerink A 2000 *J. Lumin.* **90** 123
van Dijken A, Meulenkamp E A, Vanmaekelbergh D and Meijerink A 2000 *J. Phys. Chem.* B **104** 1715
[15] Míguez H, Meseguer F, López C, Blanco Á, Moya J S, Requena J, Mifsud A and Fornés V 1998 *Adv. Mater.* **10** 480
[16] Megens M, Wijnhoven J E G J, Lagendijk A and Vos W L 1999 *J. Opt. Soc. Am.* B **16** 1403
[17] Romanov S G, Fokin A V and De La Rue R M 1999 *Appl. Phys. Lett.* **74** 1821
[18] Solovyev V G, Romanov S G, Chigrin D N and Sotomayor Torres C M 2003 *Synth. Met.* **139** 601
[19] Wu X H H, Yamilov A, Noh H, Cao H, Seelig E W and Chang R P H 2004 *J. Opt. Soc. Am.* B **21** 159
de Abajo F J G 1999 *Phys. Rev.* B **60** 6089
[20] Yamasaki T, Sumioka K and Tsutsui T 2000 *Appl. Phys. Lett.* **76** 1243
[21] Vanheusden K, Seager C H, Warren W L, Tallant D R and Voigt J A 1996 *Appl. Phys. Lett.* **68** 403
van Dijken A, Meulenkamp E A, Vanmaekelbergh D and Meijerink A 2000 *J. Lumin.* **87–89** 454
van Dijken A, Makkinje J and Meijerink A 2001 *J. Lumin.* **92** 323